

# Wound healing properties of modified silver nanoparticles and their distribution in mouse organs after topical application

Seda Keleştemur<sup>1</sup>, Ertugrul Kilic<sup>1,2</sup>, Ünal Uslu<sup>2</sup>, Alev Cumbul<sup>2</sup>, Milas Ugur<sup>1,2</sup>, Süleyman Akman<sup>3</sup>, Mustafa Culha<sup>1\*</sup>

<sup>1</sup>Department of Genetics and Bioengineering, Faculty of Engineering and Architecture, Yeditepe University, Istanbul, Turkey

<sup>2</sup>Faculty of Medicine, Yeditepe University, Istanbul, Turkey

<sup>3</sup>Department of Chemistry, Faculty of Science and Letters, Istanbul Technical University, Istanbul, Turkey

\* Corresponding author: [mculha@yeditepe.edu.tr](mailto:mculha@yeditepe.edu.tr)

## Abstract

Citrate reduced colloidal silver nanoparticles (c-AgNPs) as synthesized and modified with oligonucleotides (Oligo-AgNPs) are comparatively evaluated for their wound healing properties on animal models. The healing progress was monitored daily during nine days by measuring the wound diameter. The tissue samples from the healed regions were analyzed for epithelial damage, congestion, inflammatory cell infiltration, fibroblast proliferation, and new collagen synthesis. The c-AgNPs and Oligo-AgNPs had statically significant impact on the healing process compared to control. The histological analysis revealed that the c-AgNPs and Oligo-AgNPs improved the congestion, inflammatory cell infiltration, fibroblast proliferation and new collagen synthesis as compared to control. Although the fibroblast proliferation seems to be the same for both c-AgNPs and Oligo-AgNPs, the collagen synthesis is markedly improved with the Oligo-AgNPs. The atomic spectroscopy analysis of the samples from different tissues showed that the AgNPs applied topically to the skin does not pass through the other organs. Our data suggest that topical application of Oligo-AgNPs improve wound healing by promoting increased collagen synthesis and tissue re-modeling without any side effects.

**Keywords:** silver nanoparticles, wound healing, collagen synthesis inflammation, congestion

**Citation:** S. Keleştemur et al. Wound healing properties of modified silver nanoparticles and their distribution in mouse organs after topical application. *Nano Biomed. Eng.* 2012, 4(4), 170-176.

DOI: 10.5101/nbe.v4i4.p170-176.

## 1. Introduction

There is an increased effort to use nanoparticles (NPs) in medical applications due to their extraordinary physicochemical properties and exceptionally high surface area [1,2]. Among them, silver nanoparticles (AgNPs) are attracting considerable attention due to its biocidal properties [3-7] and positive effect on wound healing process [8,9]. The silver ions and AgNPs have been used in many consumer products and formulations to kill microorganisms for a long time. It is also used in topical formulations to prevent the infection and speed up the healing process [10-12]. Silver nitrate was used to help skin over and epithelization to remove granulation tissues from the wounds' surfaces in the 19th century [13,14]. Carl S.F. Crede used silver nitrate eye drops to heal neonatal conjunctivitis in 1881 and silver impregnated dressings to heal wounds after skin transplanting [14,15]. In 1965, Moyer presented therapy of burns using 0.5% silver nitrate [16]. Today with the increased awareness of nanotechnology-based products, the colloidal AgNPs,

synthesized with several different approaches have been started to use as biocidal agents. The popularity of the AgNPs as biocidal agent is due to the slow dissolution, which behaves as controlled release structure in one sense [17]. In addition, when the loaded Ag<sup>+</sup> concentration is considered, the AgNPs are less toxic to humans [18]. It is suggested that the biocidal effect of AgNPs is through the ionized Ag<sup>+</sup> [19]. However, its influence on wound healing is not well understood and it is still controversial whether the silver or silver based products have healing effect on wounds.

Skin wound healing process can be divided into a sequence of four time-dependent phases: coagulation and homeostasis, which is the beginning immediately after injury, inflammation, proliferation, which commences within days of the injury; and finally remodeling, which may continue more than a year [20]. As soon as coagulation starts, inflammatory cells migrate into the wound, which is characterized by the

sequential infiltration of neutrophils, macrophage and T lymphocytes. The proliferative phase generally coincides with the inflammatory phase, which is characterized by epithelial proliferation and the formation of granulation tissue at the injury site. The proliferation of the keratinocytes is stimulated by local tissue factors, then this cell migrates over the temporary extracellular matrix (ECM) and consequently re-epithelialization starts. Meanwhile, fibroblast and endothelial cells are most noticeable on the granulation tissue of dermis. Following healthy proliferation and ECM synthesis, wound healing enters the remodeling phase [21].

The healing process starts with the inflammation, and at the end of this step, the interaction between the evolving milieu of eicosanoids and present cell types ensue fibroblast synthesis of collagen and ground substances (the ratio of prostaglandin in F2 $\alpha$  and PGE2 is increased). Fibroblasts, keratinocytes and endothelial cells influx into the wounded region [22]. The proliferative phase begins with replacing neutrophils by mononuclear white blood cells. In the first week of the phase, the basic extracellular substances of granulation tissue, glycosaminoglycans, proteoglycans and collagen are produced by fibroblasts. Fibroblasts assemble collagen molecules into fibers. Collagen is the basic component of acute wound connective tissue and this progresses last six weeks [23,24]. Keratinocytes and endothelial cells produce autocrine growth factors. Buds generation with intact vessels in granulation tissue during the endothelial cells expansion contributes the angiogenesis. In the beginning of repair process, the wound is coated by fibrin cloth. This provisional matrix is replaced with granulation tissue within two days. Epithelial cells move into the wound and at the same time fibroblasts turn into myofibroblasts by contact inhibition [25]. In the maturation phase, with tensile strength, the type I collagen turns into type III collagen until the ratio of normal skin beings with 4:1. Matrix metalloproteinase collagenolysis accomplish a steady state with collagen synthesis. After 1 year of the injury, tensile strength plateaus will be nearly 80% of the original strength [26-28].

It was previously reported that the AgNPs promote wound healing by acting as a depressor for inflammation through cytokine modulation [29]. A study by Liu et al. showed that AgNPs could inhibit the production of collagen at the beginning of the wound healing process and proliferation of fibroblast [30]. In our previous *in vitro* study, we have observed increased cell proliferation with the use of oligonucleotide-silver nanoparticles (Oligo-AgNPs). In this study, we have further investigated the influence of surface chemistry of AgNPs on wound healing using animal models. The AgNPs synthesized with citrate reduction and derivatized with oligonucleotides (Oligo-AgNPs) were applied to model wounds. We found that both Oligo-AgNPs and AgNPs improved the new collagen synthesis in the injured tissue. Furthermore, our results suggested that silver does not pass through the other organs such liver, kidney

and spleen upon topical application of silver colloidal suspension.

## 2. Experimental Section

### 2.1 Synthesis and Modification of AgNPs

The modified Oligo-AgNPs are synthesized according to Culha et al [31]. Briefly, the colloidal silver nanoparticles (c-AgNPs) were prepared via the reduction of silver nitrate with sodium citrate reported by Lee and Meisel [32]. For attachment of oligonucleotide, an 8  $\mu$ L of 100  $\mu$ M thiolated oligonucleotide (5'-HS-(CH<sub>2</sub>)<sub>6</sub>-TAATGCTGAAGG-3) was added into 1 mL c-AgNPs suspension, and then this suspension was stirred for 24 h at 20 °C. At the end of 24 h, the suspension containing Oligo-AgNP was centrifuged and the supernatant was removed with a  $\mu$ -pipette. About 1 mL of distilled water was added and the centrifugation was repeated. This process was repeated three times to ensure removal of excess molecules and at the final step the Oligo-AgNPs were allowed to re-disperse by sonication for 20 min. An 8  $\mu$ L of 100  $\mu$ M thiolated oligonucleotide was added in 1 mL deionized water as a control to observe the possible effect of thiolated oligonucleotides on model ulcers.

### 2.2 Excision Wound Model and Groups

All experiments were carried out with government approval according to local guidelines for the care and use of laboratory animals. For the excision wound model, on the depilated and cleaned back of 29 adult male BalbC mice (22-26 g), the 6 full-thickness skin wounds were made as 1 cm away from the middle line and each other by using a 4.5 mm diameter punch biopsy tool under (ketamine (80-100 mg/kg i.p.), xylazine (10 mg kg<sup>-1</sup> i.p.) anesthesia. Then, these mice were randomly assigned for c-AgNPs, Oligo-AgNPs (n=7), oligonucleotide solution (n=7) and control (n=8) (Only distilled water was administered for control group) and kept in individual cages. Approximately enough to completely cover the surface of the wounds of each solution/suspension was administered topically onto the wounds on days 0 (the day the wounds are made), 2, 4, 6 and 8. The pictures of the wounds were taken on days 0, 1, 3, 5, 7 and 9 from an angle of 90 degrees against the planes of the wounds. The wound areas on the pictures measured with ImageJ 2.0 software (NIH). The healing rates are calculated with respect to the initial size of each wound and expressed as percents as to be 100% when the wound is closed completely. On day 9 the animals were sacrificed, the skin of the back covering the wound areas, liver, kidney and spleen are removed for analysis. The organs and skin covering two wounds were frozen immediately with dry ice. The test of the skin sample was placed in 10% formaldehyde for histological analysis.

### 2.3 Histology (microscopic anatomy of animal tissues)

The two skin samples from each animal were placed into 10% formaldehyde. The arbitrarily chosen six sections from each sample were taken for conventional

histological analysis. Two dyes, hematoxylin and eosin, and Masson's trichrome, were used to stain the tissue samples. The sections were analyzed for epithelial damage, congestion, inflammatory cell infiltration, fibroblast proliferation, and collagen re-construction. Epidermis and dermis thicknesses were assessed using Leica DM 4000 microscopy system and Stereo Investigator version 7.5 (Microbrightfield, Colchester, VT, USA) by averaging the measurements at five different points on each section.

**2.4 Tissue Analysis with Atomic Spectroscopy**

When a group of animals' wounds were healed, the experiment was ended. The animals were properly executed following anesthesia and the tissues from the healed wound, spleen, liver and kidney were taken from the animals for determination of Ag<sup>+</sup> ion concentrations.

Each tissue sample was weighted and digested using a 2 mL of 65% HNO<sub>3</sub> and was heated on a hot plate until the sample solutions were clear. The digested samples were allowed to cool at room temperature, filtered and diluted to 10 mL with ultra deionized water. A Varian AA 280Z Zeeman Atomic Absorption Spectrophotometer equipped with GTA 120 graphite tube atomizer was used for the measurements. A multi-element hollow cathode lamp was used as the spectral radiation source. The wavelength and spectral slit width were set to 328.1 nm and 0.5 nm. The analytical blanks were run in the same way as the samples and concentrations were determined using standard solutions prepared in the same acidic matrix. The standard solutions and the sample solutions analysis were repeated 3 times.

**2.5 Statistics**

The means of percent-healing values are compared using repeated measures of ANOVA followed by Tukey's tests. Results were expressed as means±SD. P-value of less than 0.05 was taken to indicate statistical significance.

**3. Results and discussion**

The c-AgNPs possess negative surface charge due to the adsorbed citrate ion onto them. Fig. 1A shows the UV/Vis spectrum and the TEM image of c-AgNPs. The UV/Vis spectrum typically has one absorption band at around 420 nm and the size distribution is in the range of 20-200 nm with an average size of 50 nm. Fig. 1B illustrates the surface modification of c-AgNPs with oligonucleotides. Fig. 1C show size distributions of c-AgNPs and Oligo-AgNPs. The Oligo-AgNPs were prepared by treating the hexanethiol-modified oligonucleotides. Since thiol (-SH) group has strong affinity for Ag metal surface, the oligonucleotides coat the AgNP surface [33,34]. It is demonstrated that the surface modification of AuNPs and AgNPs with a biocompatible ligand [35] or polymer [36,37] improves their biocompatibility and reduces their toxicity. In addition, we observed an increased cell proliferation of living cells upon treatment with Oligo-AgNPs in our previous study [31]. Therefore, the Oligo-

AgNPs were selected in the investigation for wound healing effect.

Fig. 2 shows photography of a model wound prepared

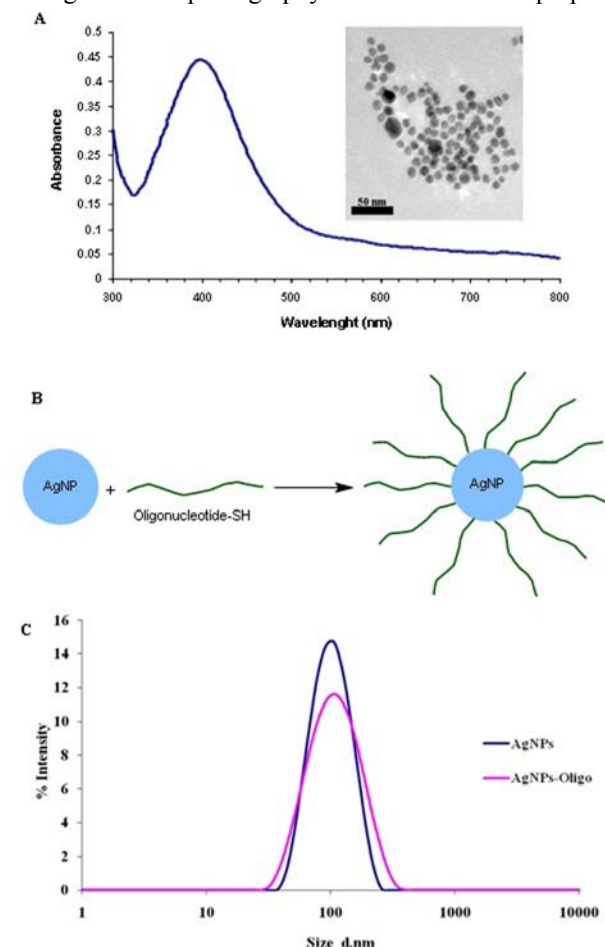


Fig. 1 UV/Vis spectrum of citrate reduced AgNP colloidal suspension and TEM image AgNPs (A). Illustration of chemical attachment of oligonucleotides onto AgNPs (B). and DLS spectrum showing size distributions of AgNPs and AgNPs-Oligo in suspension(C).

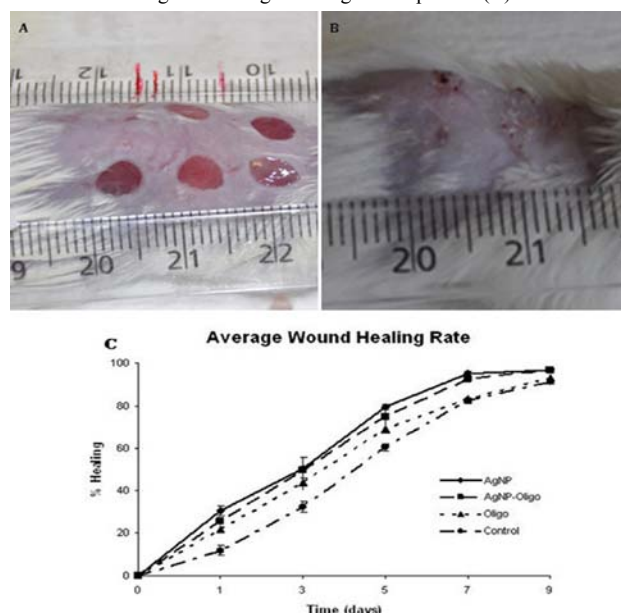


Fig. 2 A mouse with model ulcers (A), a mouse with completely healed ulcer (B), healing rates of c-AgNP, Oligo-AgNP, oligonucleotide and control groups for 9 days after the formation of wounds (C). Data represent mean± SD for all groups.

on mouse skin (A) and a completely healed wound (B), comparative average healing rate of model ulcers (C). The pictures of the wounds were taken on days 0, 1, 3, 5, 7 and 9 from an angle of 90 degrees against the planes of the wounds together with a ruler. Then, through a pixel-distance conversion by using the ruler as a reference the wound areas on the pictures measured with Image J 2.0 software (NIH) (Fig. 2C). At the end of 9-day period, more than 90% of the wound areas were closed for all groups with the control group having the lowest healing rates for all time points. For the overall process of wound healing, both c-AgNP and Oligo-AgNP treatments significantly improved the healing process when compared to the control group ( $p < 0.001$  and  $p < 0.01$ , respectively) whereas there was no statistically significant difference between oligonucleotide only and control groups. Furthermore, the healing rate of c-AgNP group was significantly higher than the oligonucleotide only group ( $p < 0.05$ ).

The sections obtained from the wounds at the end of the 9th day were analyzed for epithelial damage, congestion, inflammatory cell infiltration, fibroblast proliferation, and new collagen synthesis. The congestion and inflammatory cell infiltration are parallel processes that are observed during the cell multiplication while fibroblast proliferation

and new collagen synthesis are parallel processes that are observed during the restructuring phase of wound healing. As a result of inflammatory cell infiltration, the fibroblast proliferation and new collagen synthesis are signaled by the growth factors and cytokines. This also sends a signal for the re-synthesis of collagen fibers.

The histopathologic and morphometric evaluation of the c-AgNPs and Oligo-AgNP on wound healing are presented in Fig. 3. When the oligonucleotide only, c-AgNPs and Oligo-AgNP are compared, especially oligonucleotide only had the least damage to the epidermis. Both c-AgNPs and Oligo-AgNP signaled the congestion, inflammatory cell infiltration, fibroblast proliferation and new collagen synthesis. Although the fibroblast proliferation seems to be the same for both c-AgNPs and Oligo-AgNP, the collagen synthesis is more with c-AgNPs influencing congestion more. It seems that the inflammatory infiltration is more with the Oligo-AgNPs. Although the congestion and inflammatory cell infiltration may have a good effect on healing at the beginning, they may further delay healing process during the restructuring. The treatments of wounds with oligonucleotide only, c-AgNPs, and Oligo-AgNP result with different levels of fibroblast proliferation and congestion. Fig. 4 and 5 show histological evaluation of

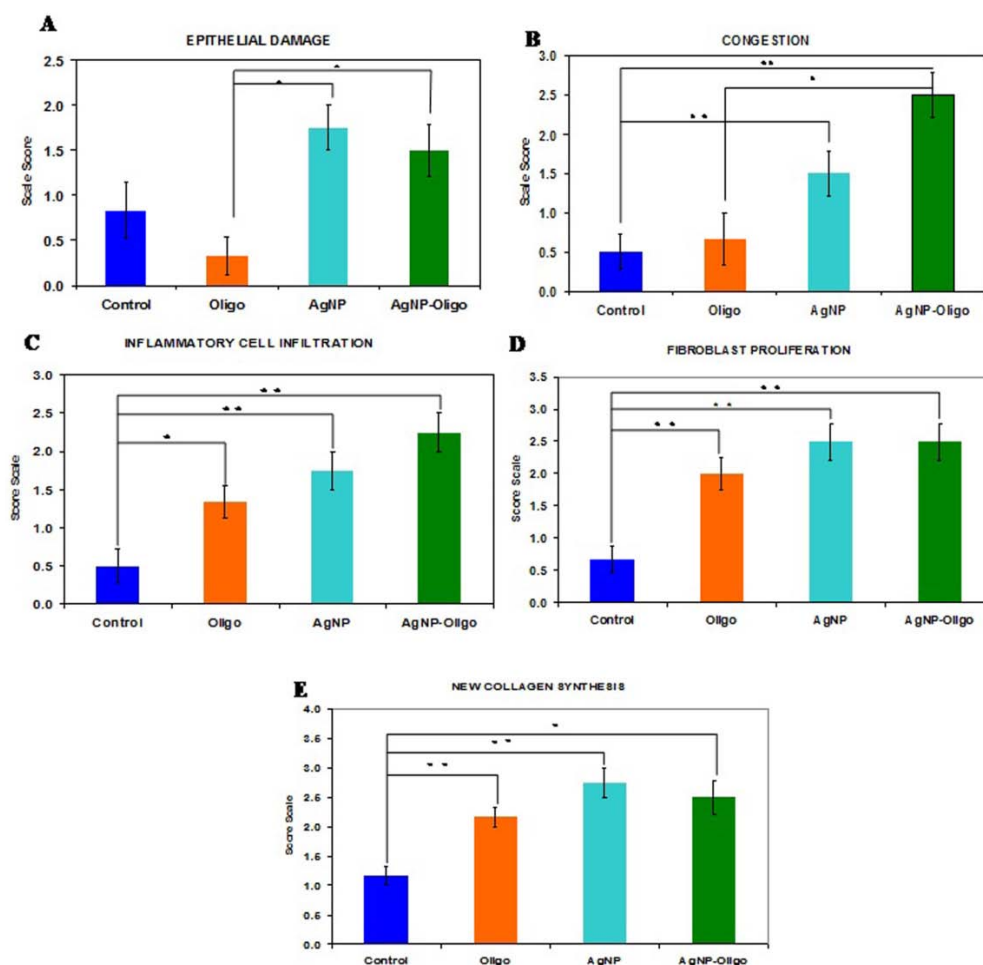


**Fig. 3** Comparison of tissue responses in terms of epithelial damage (A), congestion (B), inflammatory cell infiltration (C), fibroblast proliferation (D), and new collagen synthesis (E). Scoring: 0=None, 1=Small increase, 2= Intermediate increase, 3=Highest increase.

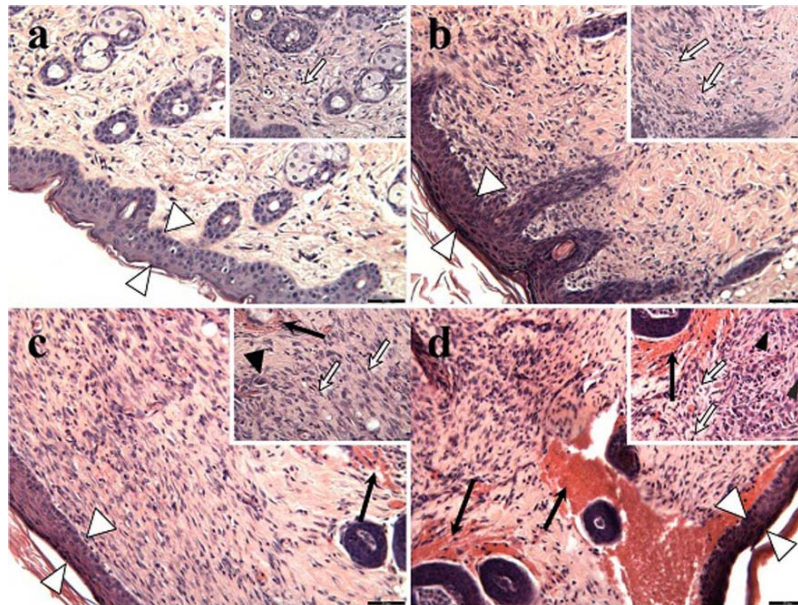


**Fig. 4** Histological evaluation of hematoxylin eosin (HE) stained tissue samples; (a) control, (b) oligonucleotide, (c) c-AgNPs, and (d) Oligo-AgNPs. Scale bars: 55  $\mu$ m in large images and 27  $\mu$ m in small images. White arrowheads show epithelial tissue, black arrowheads show macrophage, white arrows show fibroblast and black arrows show congestion.

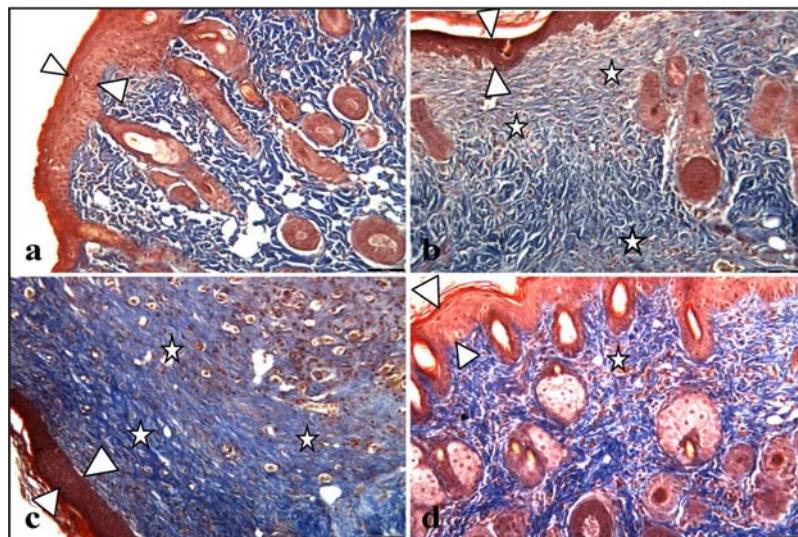


**Fig. 5** Histological evaluation of Masson's trichrom (TCM) stained tissue samples; (a) control, (b) oligonucleotide, (c) c-AgNPs, and (d) Oligo-AgNPs. Scale bars: 55  $\mu$ m for all images. White arrowheads show epithelial tissue, white stars show new collagen synthesis.

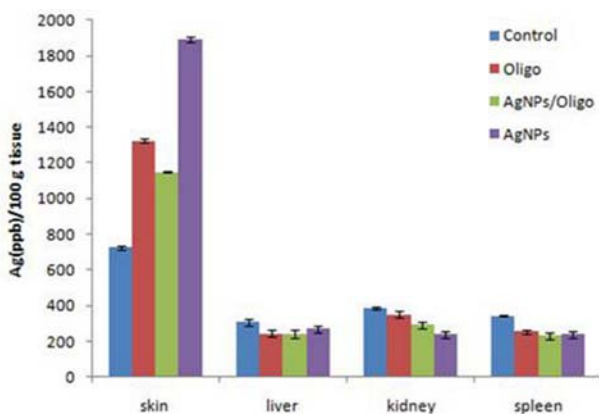


**Fig. 6** Silver concentration in skin, liver, kidney, and spleen.

the tissue samples with two different dyes, hematoxylin eosin (HE) and Masson's trichrom (TCM). In the tissue treated with oligonucleotide solution, an increase in fibroblast is apparent while treatment with Oligo-AgNP results with congestion and increased fibroblast proliferation. New collagen synthesis is highest in oligonucleotide group while it is apparent in both types of AgNPs compared to the control group.

Since  $Ag^+$  ions are toxic and cause health problems, the transport of possible dissolved  $Ag^+$  ions or AgNPs to the organs such as liver, kidney and spleen was also investigated. Fig. 6 shows the  $Ag^+$  ion concentration of the tissue samples obtained from corresponding organs. As seen, almost all of the AgNPs remain in the skin. It

is known that skin has percutaneous absorption property [38] and the reason of the higher concentrations of Ag in control and oligo groups for skin is that skin is more available to expose to contaminations from external sources. The observed concentrations in liver, kidney, and spleen are believed to be due to the natural silver uptake from water and food.

#### 4. Conclusions

The data suggests that both c-AgNPs and Oligo-AgNPs have a direct impact on wound healing. The c-AgNPs possess weakly bound citrate ions on the nanoparticle surface. However, Oligo-AgNPs have oligonucleotides tightly bound to the nanoparticle surface due to the affinity of thiol group. Although presence of oligonucleotides on the AgNP surface improves the biocompatibility, a slight decreased influence of Oligo-AgNPs on the healing process reveals that the dissolution of silver into the tissue matrix could be playing a role. Although coating the AuNP surface with a biomolecule may help to interact more thoroughly with the tissue, the delay in the dissolution of Ag metal into  $Ag^+$  reflected as a slight delay in the healing. The c-AgNPs increases the inflammation of tissue perhaps through the dissolved  $Ag^+$ . The Oligo-AgNP has a similar effect but improves the new collagen synthesis in the injured tissue. In conclusion, this study demonstrates that unmodified and modified AgNPs have similar effect on healing process with different mechanisms. Since the Oligo-AgNPs have positive effect on new collagen synthesis and tissue re-modeling, they can be used as a safer alternative to improve the wound healing without any side effects.

#### Acknowledgements

The authors greatly acknowledge the financial support of Yeditepe University, TUBITAK and TUBA-GEBIP during this study

#### References

- Mulvaney P. Surface Plasmon Spectroscopy of Nanosized Metal Particles. *Langmuir*. 1996;12: 788-800.
- Parak WJ, Gerion D, Pellegrino T et al. Biological applications of colloidal nanocrystals. *Nanotechnology*. 2003;14: R15-R27.
- Petica A., Gavrilu S, Lungu M, Buruntea N, Panzaru C. Colloidal Silver Solutions with Antimicrobial Properties. *Materials Science and Engineering*. 2008;152: 22-7.
- Gunawan C., Teoh W.Y., Marquis CP, Liffa J, Amal R. Reversible antimicrobial photoswitching in nanosilver. *Small*. 2009; 5: 341-4.
- Fernandez E.J., Garcia-Barrasa J, Laguna A, Lopez-de-Luzuriaga JM, Monge M, Torres C. The preparation of highly active antimicrobial silver nanoparticles by an organometallic approach. *Nanotechnology*. 2008; 19: 185602.
- Morones JR, Elechiguerra JL, Camacho A et al. The bactericidal effect of silver nanoparticles. *Nanotechnology*. 2005; 16: 2346-53.
- Vasilev K, Sah V, Anselme K et al. Tunable antibacterial coatings that support mammalian cell growth. *Nano Letter*. 2009; 10: 202-7.
- Wright JB, Lam K, Buret A, Olson ME, Burrell RE. Early healing events in a porcine model of contaminated wounds: effects of nanocrystalline silver on matrix metalloproteinases, cell apoptosis, and healing. *Wound Repair Regen*. 2007; 10: 141-51.
- Huang Y, Li X, Liao Z et al. A randomized comparative trial between Acticoat and SD-Ag in the treatment of residual burn wounds, including safety analysis. *Burns*. 2007; 33: 161-6.
- Carlson C, Hussain SM, Schrand AM et al. Unique cellular interaction of silver nanoparticles: size-dependent generation of reactive oxygen species. *J Phys Chem*. 2008; 112: 13608-13619.
- Asharani PV, Mun GLK, Hande MP, Valiyaveetil S. Cytotoxicity and genotoxicity of silver nanoparticles in human cells. *ACS Nano*. 2008; 3: 279-290.
- Sondi I, Salopek-Sondib B. Silver nanoparticles as antimicrobial agent: a case study on *E. coli* as a model for Gram-negative bacteria. *J Colloid Interface Sci*. 2004; 275: 177-182.
- Castellano JJ, Shafii SM, Ko F et al. Comparative evaluation of silver-containing antimicrobial dressings and drugs. *Int Wound J*. 2007; 4: 114-122.
- Klasen HJ. A historical review of the use of silver in the treatment of burns. Part I early uses. *Burns*. 2000; 26: 117-30.
- Landsdown ABG. Silver I: its antibacterial properties and mechanism of action. *J Wound Care*. 2002; 11: 125-38.
- Moyer CA, Brentano L, Gravens DL, Margraf HW, Monafu WW. Treatment of large human burns with 0.5% silver nitrate solution. *Arch Surg*. 1965; 90: 812-67.
- Fan FR, Bard AJ. Imaging of biological macromolecules on mica in humid air by scanning electrochemical microscope. *Proc Natl Acad Sci USA*. 1999; 96: 14222-7.
- Foldbjerg R, Olesen P, Hougaard M, Dang DA, Hoffmann HJ, Autrup H. PVP-coated silver nanoparticles and silver ions induce reactive oxygen species, apoptosis and necrosis in THP-1 monocytes. *Toxicol Lett*. 2009; 190: 156-62.
- Hwang ET, Lee JH, Chae YJ et al. Analysis of the toxic mode of action of silver nanoparticles using stress-specific bioluminescent bacteria. *Small*. 2008; 4: 746-50.
- Guo S, DiPietro LA. Factors affecting wound healing. *J Dent Res*. 2010; 89: 219-29.
- Velnar T, Bailey T, Smrkolj V. The wound healing process: an overview of the cellular and molecular mechanism. *J Int Med Res*. 2009; 37: 1528-42.
- De la Torre JI, Chambers JA. Wound healing, chronic wounds. *Evidence* 2008.
- Robson MC. The role of growth factors in the healing of chronic wounds. *Wound Repair Regen*. 1997; 5: 12-7.
- Robson MC, Burns BF, Phillips LG. Wound repair: principles and applications. In: Ruberg RL (Ed), Smith DJ (Ed). *Plastic surgery: a core curriculum*. St. Louis, MO: Mosby-Year Book, 1994; 3-30.
- Chin GA, Diegelmann RF, Schultz GS. Cellular and molecular regulation of wound healing. *Wound Heal*. 2005; 2005: 17-39.
- Robson MC, Hill DP, Woodske ME, Steed DL. Wound healing trajectories as predictors of effectiveness of therapeutic agents. *Arch Surg*. 2000; 135: 773-7.
- Steed DL. The role of growth factors in wound healing. *Surg Clin North Am*. 1997; 77: 575-86. Doi: 10.1016/S0039-6109(05)70569-7.
- Eaglstein WH, Falanga V. Chronic wound. *Surg Clin North Am*. 1997; 77: 689-700.
- Tian J, Wong KK, Ho CM et al. Topical delivery of silver nanoparticles promotes wound healing. *ChemMedChem*. 2007; 2: 129-36.
- Liu X, Lee P, Ho C, Lui VCH., Chen Y., Che C., Tam PKH., Wong KKY. Silver Nanoparticles Mediate Differential Responses in Keratinocytes and Fibroblasts during Skin Wound Healing. *ChemMedChem*. 2010; 5: 468-75.
- Sur I, Cam D, Kahraman M, Baysal A, Culha M. Interaction of multifunctional silver nanoparticles with living cells. *Nanotechnology*. 2010; 21: 175104.
- Lee PC, Meisel D. Adsorption and surface-enhanced Raman of dyes on silver and gold sols. *J Phys Chem*. 1982; 86: 3391.
- Schwaha K, Spencer ND, Lambert RM. A single crystal study of the initial stages of silver sulphidation: The chemisorption and reactivity of molecular sulphur (S<sub>2</sub>) on Ag (111). *Surface Science*. 1979; 81: 273-84.
- Rovida G, Pratesi F. Sulfur overlayers on the low-index faces of silver. *Surface Science*. 1981; 104: 609-24.
- Huang JT, Hou SY, Fang SB, Yu HW, Lee HC, Yang CZ. Development of a biochip using antibody-coated gold nanoparticles to detect specific bioparticles. *J Ind Microbiol Biotechnol*. 2008; 35: 1377-85.
- Quaroni L, Chumanov G. Preparation of Polymercoated Functionalized Silver Nanoparticles. *J Am Chem Soc*. 1999; 121: 10642-3.
- Mandal TK, Fleming MS, Walt DR. Preparation of Polymer Coated Gold Nanoparticles by Surface-Confined Living Radical Poly-

<http://nanobe.org>

- merization at Ambient Temperature. *Nano Lett.* 2002; 2: 3-7.
- 38 Lansdown AB, Sampson B. Dermal toxicity and percutaneous absorption of cadmium in rats and mice. *Lab Anim Sci.* 1996; 46: 549-54.

**Copyright:**(c) 2012 S. Keleştemur et al. This is an open-access article distributed under the terms of the Creative Commons Attribution License, which permits unrestricted use, distribution, and reproduction in any medium, provided the original author and source are credited.